

Macroscopic fluctuation theory of local time in lattice gases

Naftali R. Smith^a, Baruch Meerson^b

^a*Department of Environmental Physics, Blaustein Institutes for Desert Research,
Ben-Gurion University of the Negev, Sede Boqer Campus, 8499000, Israel*

^b*Racah Institute of Physics, Hebrew University of Jerusalem, Jerusalem, 91904, Israel*

Abstract

The local time in an ensemble of particles measures the amount of time the particles spend in the vicinity of a given point in space. Here we study fluctuations of this quantity, that is of the empirical time average $R = \int_0^T \rho(x=0, t) dt$ of the density $\rho(x=0, t)$ at the origin for an initially uniform one-dimensional diffusive lattice gas. We consider both the quenched and annealed initial conditions and employ the Macroscopic Fluctuation Theory (MFT). For a gas of non-interacting random walkers (RWs) the MFT yields exact large-deviation functions of R , which are closely related to the ones recently obtained by Burennev *et al.* (2023) using microscopic calculations for non-interacting Brownian particles. Our MFT calculations, however, additionally yield the most likely history of the gas density $\rho(x, t)$ conditioned on a given value of R . Furthermore, we calculate the variance of the local time fluctuations for arbitrary particle- or energy-conserving diffusive lattice gases. Better known examples of such systems include the simple symmetric exclusion process, the Kipnis-Marchioro-Presutti model and the symmetric zero-range process. Our results for the non-interacting RWs can be readily extended to a step-like initial condition for the density.

1. Introduction

Fluctuations in spatially extended macroscopic systems are a central paradigm of interest in statistical mechanics. Macroscopic fluctuations can

Email addresses: naftalismsith@gmail.com (Naftali R. Smith),
meerson@mail.huji.ac.il (Baruch Meerson)

be quantified by considering different observables, such as the current of mass or energy, activity, *etc.* One useful measure of fluctuations is the “local time”, *i.e.* the total time spent by the systems’s particles at or around a specified point in space. The local time has many applications in different fields. For example, consider chemical or biological reactions, in which a receptor’s activity is proportional to the time during which the reactants stay in its vicinity. Then the yield of the product is given by the local time spent by the reactants at the location of the receptor [1–4]. The local time can also be viewed as the occupation (or residence) time within a given spatial domain, in the limit where the size of the domain vanishes [5–11].

The local time has been studied extensively for single-particle systems [12–21]. Very recently Burennev *et al.* [22] considered a many-body system consisting of noninteracting Brownian particles on the line, whose initial density is uniform on the negative half-line and zero on the positive one. They studied the probability distribution of the local time at the origin, and focused on the large-deviation regime and on the (ever-lasting) effect of the type of initial condition – quenched (that is deterministic) or annealed (random).

In this work, we extend the results of Ref. [22] in two directions:

(i) By applying the macroscopic fluctuation theory (MFT) (see Ref. [23] for a review), to the gas of noninteracting random walkers (RWs) on a lattice, we calculate exact large-deviation functions of R and show that they are closely related to the ones calculated by Burennev *et al.* (2023) using a microscopic approach. In addition we study, in the quenched and annealed cases, the optimal (*i.e.* most likely) history of the gas density, which dominates the probability of observing a given value of the local time R . The optimal histories, or paths, are interesting quantities because they provide important insights into the physical mechanisms behind large deviations. The optimal paths can be observed in simulations [24–30] and, in principle, in experiments. In particular, we find that, in the annealed case, the optimal gas density history obeys a time-reversal symmetry around $t = T/2$.

(ii) Employing the MFT, we calculate the variance of R for a broad class of *interacting* particle- or energy-conserving diffusive lattice gases with arbitrary diffusivity and mobility [31–34]. Among the better known examples of such gases are the simple symmetric exclusion process (SSEP), the Kipnis-Marchioro-Presutti (KMP) model [31–33, 35] and the symmetric zero-range process (ZRP) [31–34, 36, 37]. Additional examples include the Katz-Lebowitz-Spohn (KLS) model [38, 39], the Kob-Andersen kinetically-

constrained model [40, 41], the repulsion process [42], a family of “strong particle” models, the facilitated exclusion process, the exclusion process with avalanches, and other models, see Ref. [43] and references therein.

The MFT is based on a saddle-point evaluation of the path integral which provides a coarse-grained description of the (noisy) dynamics of the gas density. The ensuing minimization procedure gives rise to saddle-point equations which solution yields the optimal gas density history. We assume an initially uniform density on the entire real line. This setting is slightly simpler, than the step-function initial density profile considered in Ref. [22]. We show however that, for the non-interacting RWs, the two local-time distributions for the two initial conditions are simply related.

The rest of the paper is organized as follows. Section 2 starts with a well-known coarse-grained description of diffusive lattice gases [31] and presents the MFT formulation of the local time statistics problem for such gases. In Sec. 3 we determine the full probability distribution of the local time for noninteracting random walkers (RWs), as well as the optimal histories as described above, for the quenched and annealed initial conditions, and compare our results for the distribution of local time with those of Ref. [22]. In Sec. 4 we calculate the variance of the distribution of local time for interacting lattice gases with arbitrary diffusivity and mobility. In Sec. 5 we briefly summarize and discuss our results.

2. Model, basic definitions and governing equations

A rigorous coarse-grained description of stochastic dynamics of diffusive lattice gases is provided by the fluctuating hydrodynamics formalism. It involves a Langevin equation which effectively accounts, on large scales and at long times, for the contribution of the shot noise to the particle flux [31]. In one dimension this equation reads

$$\partial_t \rho + \partial_x j = 0, \tag{1}$$

where

$$j = -D(\rho)\partial_x \rho - \sqrt{\sigma(\rho)}\eta. \tag{2}$$

Here $\rho(x, t)$ and $j(x, t)$ are the density of particles and current respectively, and $\eta = \eta(x, t)$ is a white, Gaussian noise, satisfying

$$\langle \eta(x, t) \rangle = 0, \quad \langle \eta(x, t)\eta(x', t') \rangle = \delta(x - x')\delta(t - t'). \tag{3}$$

Model	$D(\rho)$	$\sigma(\rho)$	$F(\rho)$
RWs	1	2ρ	$\rho \ln \rho - \rho$
SSEP	1	$2\rho(1 - \rho)$	$\rho \ln \rho + (1 - \rho) \ln(1 - \rho)$
KMP	1	$2r^2$	$-\ln r$
ZRP	$\alpha'(\rho)$	$2\alpha(\rho)$	$\int^\rho \ln \alpha(\rho) d\rho$

Table 1: Transport coefficients $D(\rho)$ and $\sigma(\rho)$ and the free energy density $F(\rho)$ for the non-interacting RWs and for three interacting particle systems: the SSEP, the KMP model and the ZRP. Here $\alpha(\rho)$ is the microscopic rate of the ZRP, and it is assumed that $\alpha'(\rho) > 0$.

The transport coefficients $D(\rho)$ and $\sigma(\rho)$ are the diffusivity and mobility of the gas, respectively, which are determined by the microscopic dynamics of the specific model. Table 1 presents these transport coefficient, as well as the free energy density $F(\rho)$, which is discussed below, for the RWs, the SSEP, the KMP and the ZRP.

We suppose that at $t = 0$ the gas occupies the entire x -axis, and the gas density $\rho(x, t = 0) = n_0$ is uniform. We will consider both quenched, and annealed initial conditions. Following Ref. [22], we are interested in the full probability distribution $\mathcal{P}(R)$ of the “local time”, that is the empirical time average of the density at a point which we can choose to be the origin:

$$R = \frac{1}{T} \int_0^T \rho(x = 0, t) dt. \quad (4)$$

At long times $T \gg 1$ the noise term in Eq. (2) becomes effectively weak, as shown in Appendix A. Therefore, $\mathcal{P}(R)$ can be approximately determined via a saddle-point evaluation of the path integral corresponding to Eqs. (1), (2) and (4). The action minimization procedure, which we perform explicitly in Appendix A, yields the MFT equations which can be presented in a Hamiltonian form. In rescaled variables $t/T \rightarrow t$, $x/\sqrt{T} \rightarrow x$, they read

$$\partial_t q = \partial_x [D(q) \partial_x q - \sigma(q) \partial_x p], \quad (5)$$

$$\partial_t p = -D(q) \partial_x^2 p - \frac{1}{2} \sigma'(q) (\partial_x p)^2 - \Lambda \delta(x), \quad (6)$$

where $q(x, t)$ – a deterministic field – is the optimal history of the density $\rho(x, t)$, $p(x, t)$ is the “conjugate momentum” density [which is related to the optimal history of the noise $\xi(x, t)$], and Λ is a Lagrange multiplier which accounts for the integral constraint (4) and is ultimately expressed via R . As

one can see, Eq. (6) contains a source term $-\Lambda\delta(x)$ which is specific to the problem of local time statistics.

To complete the definition of the problem, the MFT equations must be supplemented with boundary conditions in space and time. The spatial boundary conditions are

$$q(|x| \rightarrow \infty, t) = n_0, \quad p(|x| \rightarrow \infty, t) = 0. \quad (7)$$

Since the gas density is unspecified at $t = 1$, this yields the “free” boundary condition

$$p(x, t = 1) = 0. \quad (8)$$

The initial condition at $t = 0$ depends on the way in which the initial density is chosen. In the quenched case, the initial density is deterministically uniform, and thus

$$q(x, t = 0) = n_0. \quad (9)$$

In the annealed case, the initial condition is random with *average* density n_0 , corresponding to the assumption that the system had a sufficient time to equilibrate prior to $t = 0$. This leads to the initial condition

$$p(x, t = 0) = \mathcal{F}'[q(x, 0)] \quad (10)$$

for the MFT equations, where

$$\mathcal{F}(r) = F(r) - F(n_0) - F'(n_0)(r - n_0), \quad (11)$$

see *e.g.* Ref. [44]. The equilibrium free energy density of the gas $F(r)$ is related to the diffusivity and mobility coefficients via $F''(r) = 2D(r)/\sigma(r)$.

Once the MFT problem is solved, the long-time probability distribution $\mathcal{P}(R)$ can be obtained, in the leading order, by evaluating the action along the optimal path. This leads to a universal large- T scaling behavior

$$\mathcal{P}(R) \sim e^{-\sqrt{T}s(R)}. \quad (12)$$

The large-deviation function $s(R)$ depends on the type of initial condition – quenched or annealed – and, through $D(\rho)$ and $\sigma(\rho)$, on the particular lattice gas model.

For the quenched case, $s(R)$ can be calculated by evaluating the dynamical action $s(R) = s_{\text{dyn}}(R)$ where

$$s_{\text{dyn}}(R) = \frac{1}{2} \int_0^1 dt \int_{-\infty}^{\infty} dx \sigma(q) (\partial_x p)^2. \quad (13)$$

In the annealed case, one should also take into account the “cost” $s_{\text{in}}(R)$ of creating the optimal initial density profile:

$$s_{\text{in}}(R) = \int_{-\infty}^{\infty} dx \mathcal{F}[q(x, 0)] , \quad (14)$$

so that the total action is given by $s = s_{\text{in}} + s_{\text{dyn}}$. Full details of the derivation of the MFT formulation are given in [Appendix A](#).

In practice, the evaluation of the double integral in Eq. (13) can be difficult. It is often convenient, therefore, to employ a useful shortcut in the form of the relation

$$\frac{ds}{dR} = \Lambda , \quad (15)$$

which follows from the fact that R and Λ are conjugate variables, see *e.g.* Ref. [46].

3. Complete statistics of the local time for noninteracting RWs

3.1. General

For noninteracting RWs, the MFT equations (5) and (6) read

$$\partial_t q = \partial_x^2 q - \partial_x(2q\partial_x p) , \quad (16)$$

$$\partial_t p = -\partial_x^2 p - (\partial_x p)^2 - \Lambda\delta(x) . \quad (17)$$

Applying the Hopf-Cole canonical transformation $Q = qe^{-p}$ and $P = e^p$ to Eqs. (16) and (17), we obtain the linear, decoupled equations

$$\partial_t Q = \partial_x^2 Q + \Lambda Q\delta(x) , \quad (18)$$

$$\partial_t P = -\partial_x^2 P - \Lambda P\delta(x) . \quad (19)$$

The boundary condition (8) becomes

$$P(x, t = 1) = 1 . \quad (20)$$

The quenched initial condition (9) becomes

$$Q(x, t = 0)P(x, t = 0) = n_0 . \quad (21)$$

By virtue of Eq. (11) and the relation $F'(r) = \ln r$ (see the first line of Table 1), the annealed initial condition (10) reads

$$p(x, t = 0) = \ln \frac{q(x, t = 0)}{n_0}. \quad (22)$$

In the Hopf-Cole variables Eq. (22) becomes very simple:

$$Q(x, t = 0) = n_0. \quad (23)$$

We now proceed to solve the MFT problem in the Hopf-Cole variables. We first determine $P(x, t)$ by solving Eq. (19) backwards in time, with “final” condition (20). Let us denote $f(t) \equiv P(0, t)$, and reverse time, $\tilde{t} = 1 - t$, so that Eq. (19) becomes

$$\partial_{\tilde{t}} P(x, \tilde{t}) = \partial_x^2 P(x, \tilde{t}) + \Lambda f(\tilde{t}) \delta(x) \quad (24)$$

and Eq. (20) becomes the initial condition $P(x, \tilde{t} = 0) = 1$. Equation (24) is an inhomogeneous linear heat equation with a source term $\Lambda f(\tilde{t}) \delta(x)$, and its formal solution is given by

$$P(x, \tilde{t}) = 1 + \frac{\Lambda}{\sqrt{4\pi}} \int_0^{\tilde{t}} d\tau \frac{f(\tau)}{\sqrt{\tilde{t} - \tau}} e^{-x^2/4(\tilde{t} - \tau)}. \quad (25)$$

Setting $x = 0$ in Eq. (25) yields an integral equation for the unknown $f(\tilde{t})$,

$$\frac{\Lambda}{\sqrt{4\pi}} \int_0^{\tilde{t}} d\tau \frac{f(\tau)}{\sqrt{\tilde{t} - \tau}} = f(\tilde{t}) - 1, \quad (26)$$

which is known as the Abel’s equation of the second kind. Its solution, already in the original time t , is [45]

$$f(1 - t) \equiv P(x = 0, t) = e^{\frac{\Lambda^2(1-t)}{4}} \operatorname{erfc} \left(-\frac{\Lambda\sqrt{1-t}}{2} \right), \quad (27)$$

where $\operatorname{erfc}(z) = 1 - (2/\sqrt{\pi}) \int_0^z e^{-t^2} dt$ is the complementary error function. Plugging Eq. (27) into Eq. (25), one obtains an integral expression for $P(x, t)$. We now continue to solve the MFT problem, first for the annealed case, and then for the quenched case which is a little more complicated.

3.2. Annealed initial condition

In the annealed case, the calculation of $Q(x, t)$ is very similar to that of $P(x, t)$. One notices that Eq. (18) with the initial condition (23) is almost identical to Eq. (24) with the initial condition $P(x, \tilde{t} = 0) = 1$. Indeed, for $n_0 = 1$ the two problems are identical, but since the equations are linear, the solution will simply be proportional to n_0 . In particular, we immediately obtain, by analogy with Eq. (27), that

$$Q(x = 0, t) = n_0 e^{\Lambda^2 t/4} \operatorname{erfc} \left(-\frac{\Lambda \sqrt{t}}{2} \right). \quad (28)$$

Using this result, one can obtain an integral expression for $Q(x, t)$ at arbitrary t but, as we now show, this is unnecessary for the purpose of calculating the large-deviation function. Indeed, from Eqs. (27) and (28) one finds that the density at the origin at times $0 \leq t \leq 1$ is given by

$$q(x = 0, t) = Q(0, t)P(0, t) = n_0 e^{\Lambda^2 t/4} \operatorname{erfc} \left(-\frac{\Lambda \sqrt{1-t}}{2} \right) \operatorname{erfc} \left(-\frac{\Lambda \sqrt{t}}{2} \right). \quad (29)$$

Plugging Eq. (29) into the rescaled version of Eq. (4), *i.e.* $R = \int_0^1 q(x = 0, t) dt$, we obtain

$$R(\Lambda) = n_0 e^{\Lambda^2/4} \int_0^1 dt \operatorname{erfc} \left(-\frac{\Lambda \sqrt{1-t}}{2} \right) \operatorname{erfc} \left(-\frac{\Lambda \sqrt{t}}{2} \right). \quad (30)$$

Evaluating the integral (see Appendix B), we obtain

$$R(\Lambda) = \frac{2n_0}{\Lambda^2} \left\{ e^{\Lambda^2/4} (\Lambda^2 - 2) \left[\operatorname{erf} \left(\frac{\Lambda}{2} \right) + 1 \right] + \frac{2\Lambda}{\sqrt{\pi}} + 2 \right\}. \quad (31)$$

Now we employ Eq. (15) to calculate the large deviation function $s(R)$. Applying the chain rule, we find

$$\frac{1}{n_0} \frac{ds}{d\Lambda} = \frac{\Lambda}{n_0} \frac{dR}{d\Lambda} = \frac{e^{\Lambda^2/4} (\Lambda^4 - 2\Lambda^2 + 8) \left[\operatorname{erf} \left(\frac{\Lambda}{2} \right) + 1 \right] + \frac{2}{\sqrt{\pi}} (\Lambda^3 - 4\Lambda - 4\sqrt{\pi})}{\Lambda^2}. \quad (32)$$

Integrating Eq. (32) with respect to Λ with the additional condition $s|_{\Lambda=0} = 0$, we obtain

$$\frac{s}{n_0} = \frac{2 \left\{ e^{\Lambda^2/4} (\Lambda^2 - 4) \left[\operatorname{erf} \left(\frac{\Lambda}{2} \right) + 1 \right] + 4 \right\}}{\Lambda} + \frac{8}{\sqrt{\pi}}. \quad (33)$$

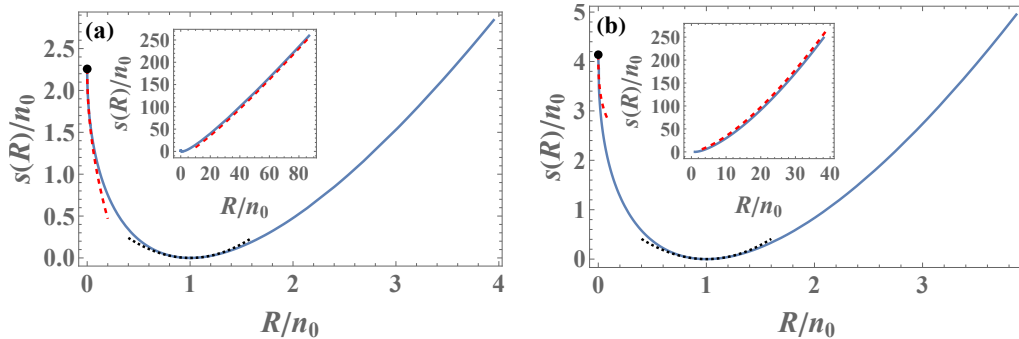


Figure 1: Solid lines: $s(R)/n_0$ vs. R/n_0 for the annealed (a) and quenched (b) initial conditions. The dashed and dotted lines in the main plots and the dashed lines in the insets correspond to the $R \ll n_0$, $R \simeq n_0$ and $R \gg n_0$ asymptotic behaviors, respectively, see Eqs. (34) and (42).

Equations (31) and (33) give the rate function $s(R)$ for the annealed initial condition in a parametric form¹.

The asymptotic behaviors of $s(R)$ are given by

$$s(R) \simeq \begin{cases} 4n_0/\sqrt{\pi} - 4\sqrt{R/n_0}, & R \ll n_0, \\ \frac{3\sqrt{\pi}}{8n_0} (R - n_0)^2, & |R - n_0| \ll n_0, \\ R \left[2\sqrt{\ln\left(\frac{R}{4n_0}\right)} - \frac{1}{\sqrt{\ln\left(\frac{R}{4n_0}\right)}} \right], & R \gg n_0, \end{cases} \quad (34)$$

and they are plotted, alongside with the exact $s(R)$, in Fig. 1 (a). For completeness, we derive these asymptotics in Appendix C.

At $R = 0$, the first line of Eq. (34) coincides with the action, corresponding to the (two-sided) survival probability of an absorbing wall, located at $x = 0$, for the annealed initial condition. The corresponding one-sided survival action, $2n_0/\sqrt{\pi}$, has been known for some time [47].

The optimal history of the gas density, conditioned on a specified R , can be determined from the relation $q(x, t) = Q(x, t)P(x, t)$, where Q and P are found as described above. Using the relation $Q(x, t) = n_0P(x, 1 - t)$ we

¹One can establish a simple connection between the large-deviation function $s(R)$, as described by Eqs. (31) and (33), and the large deviation function for the step initial condition, determined in Ref. [22]. This connection is presented in Sec. 3.4.

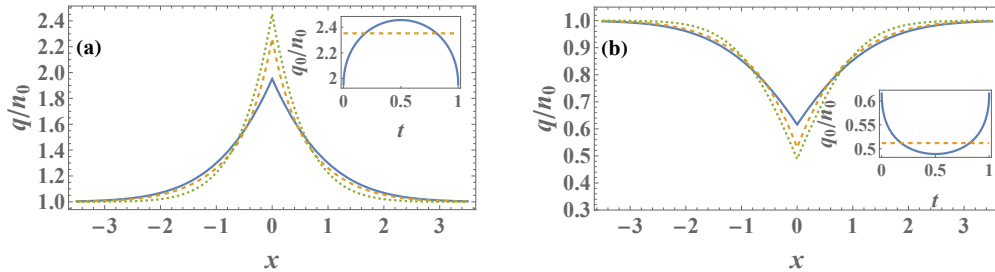


Figure 2: The optimal density history of the noninteracting RWs, for the annealed initial condition, as a function of x at times $t = 0, 0.1$ and 0.5 (solid, dashed and dotted lines, respectively) for $\Lambda = 1$ (a) and $\Lambda = -1$ (b). At times $1/2 \leq t \leq 1$, $q(x, t)$ is given by the time-reversal symmetry relation $q(x, t) = q(x, 1 - t)$. Insets: The optimal densities at the origin, $q_0(t) = q(x = 0, t)$ (solid lines) and their time average values R (dashed lines).

find that the optimal history of the density $q(x, t)$ satisfies a time-reversal symmetry $q(x, t) = q(x, 1 - t)$ around $t = 1/2$. Optimal trajectories for $\Lambda = 1$ and $\Lambda = -1$, corresponding to $R/n_0 = 2.3520\dots$ and $R/n_0 = 0.51186\dots$, respectively, are plotted in Fig. 2. Notice the nontrivial shape of the optimal density profile already at $t = 0$. Also noticeable is a corner singularity of the density profile at $x = 0$ which is present at all times.

3.3. Quenched initial condition

For the quenched case, one solves Eq. (19) exactly as in the annealed case. However, solving Eq. (18) becomes rather more complicated due to the initial condition (21). This, in turn, makes it difficult to evaluate R as a function of Λ directly.

We therefore employ another trick which simplifies the calculation considerably. We use the property

$$\begin{aligned} \frac{d}{dt} \int_{-\infty}^{\infty} pq \, dx &= \int_{-\infty}^{\infty} (p \partial_t q + q \partial_t p) \, dx = \\ &= \int_{-\infty}^{\infty} [q (\partial_x p)^2 - \Lambda \delta(x) q] \, dx, \end{aligned} \quad (35)$$

which follows from the MFT equations (16) and (17) after performing spatial integrations by parts (using the boundary conditions at $|x| \rightarrow \infty$). From

Eq. (35), it follows that the action (13) can be recast as

$$\begin{aligned}
s &= \int_0^1 dt \int_{-\infty}^{\infty} dx q (\partial_x p)^2 \\
&= \int_0^1 dt \left[\Lambda q(0, t) + \frac{d}{dt} \int_{-\infty}^{\infty} pq dx \right] \\
&= \Lambda R + \left[\int_{-\infty}^{\infty} pq dx \right]_{t=0}^{t=1} \\
&= \Lambda R - n_0 \int_{-\infty}^{\infty} p(x, t=0) dx, \tag{36}
\end{aligned}$$

where in the last equality we used the temporal boundary conditions (8) and (9). It therefore becomes useful to define the scaled cumulant generating function (SCGF)

$$\mu(\Lambda) = \Lambda R(\Lambda) - s(\Lambda) = n_0 \int_{-\infty}^{\infty} p(x, t=0) dx, \tag{37}$$

which is the Legendre transform of $s(R)$.

We now proceed to calculate $\mu(\Lambda)$. For this, it is necessary first to calculate $p(x, t=0) = \ln P(x, t=0)$. Plugging (27) into (25), we obtain, at $t=0$,

$$P(x, t=0) = 1 + \frac{\Lambda}{\sqrt{4\pi}} \int_0^1 d\tau \frac{\exp\left(\frac{\Lambda^2\tau}{4} - \frac{x^2}{4(1-\tau)}\right) \operatorname{erfc}\left(-\frac{\Lambda\sqrt{\tau}}{2}\right)}{\sqrt{1-\tau}}. \tag{38}$$

This integral turns out to be solvable, and the result is

$$P(x, t=0) = \operatorname{erf}\left(\frac{|x|}{2}\right) + e^{\Lambda(\Lambda-2|x|)/4} \operatorname{erfc}\left(\frac{|x|-\Lambda}{2}\right). \tag{39}$$

We were unable to show this fact analytically, but we verified it numerically². Plugging the logarithm of the expression (39) into Eq. (37), we obtain

$$\begin{aligned}
\mu(\Lambda) &= 2n_0 \int_0^{\infty} p(x, t=0) dx \\
&= 2n_0 \int_0^{\infty} \ln \left[\operatorname{erf}\left(\frac{x}{2}\right) + e^{\Lambda(\Lambda-2x)/4} \operatorname{erfc}\left(\frac{x-\Lambda}{2}\right) \right] dx. \tag{40}
\end{aligned}$$

²The right-hand side of Eq. (39) is closely related to expressions which appear in Ref. [22], and this is how we were able to guess the solution to this integral.

Using this result, we obtain $s(R)$ in a parametric form by performing the Legendre transform,

$$R(\Lambda) = \frac{d\mu}{d\Lambda} = 2n_0 \int_0^\infty \frac{e^{-x^2/4} \left[2 - \sqrt{\pi} e^{(x-\Lambda)^2/4} (x-\Lambda) \operatorname{erfc} \left(\frac{x-\Lambda}{2} \right) \right]}{2\sqrt{\pi} \left[\operatorname{erf} \left(\frac{x}{2} \right) + e^{\Lambda(\Lambda-2x)/4} \operatorname{erfc} \left(\frac{x-\Lambda}{2} \right) \right]} dx$$

and

$$\begin{aligned} s(\Lambda) &= \Lambda R - \mu \\ &= 2n_0 \int_0^\infty \left\{ \frac{\Lambda e^{-x^2/4} \left[2 - \sqrt{\pi} e^{(x-\Lambda)^2/4} (x-\Lambda) \operatorname{erfc} \left(\frac{x-\Lambda}{2} \right) \right]}{2\sqrt{\pi} \left[\operatorname{erf} \left(\frac{x}{2} \right) + e^{\Lambda(\Lambda-2x)/4} \operatorname{erfc} \left(\frac{x-\Lambda}{2} \right) \right]} \right. \\ &\quad \left. - \ln \left[\operatorname{erf} \left(\frac{x}{2} \right) + e^{\Lambda(\Lambda-2x)/4} \operatorname{erfc} \left(\frac{x-\Lambda}{2} \right) \right] \right\} dx. \end{aligned} \quad (41)$$

An analysis very similar to that performed in [22] yields the asymptotic behaviors

$$s(R) \simeq \begin{cases} 4n_0 \left(\phi_\infty - \sqrt{-\frac{R}{2n_0} \ln \frac{R}{n_0}} \right), & R \ll n_0, \\ \frac{3\sqrt{\pi} n_0}{8(2-\sqrt{2})} \left(\frac{R}{n_0} - 1 \right)^2, & |R - n_0| \ll n_0, \\ \frac{2^{5/2} R^{3/2}}{3^{3/2} n_0^{1/2}}, & R \gg n_0, \end{cases} \quad (42)$$

where $\phi_\infty = -\int_0^\infty \ln \operatorname{erf}(z) dz = 1.03442\dots$. Figure 1 (b) shows these asymptotics alongside with the exact large-deviation function $s(R)$.

At $R = 0$, the first line of Eq. (42) coincides with the two-sided survival probability of an absorbing wall at $x = 0$ for the quenched initial condition. The twice as small one-sided survival action, $2n_0\phi_\infty$, was calculated in Ref. [48].

An analytical calculation of the optimal density history $q(x, t)$ here is more difficult than in the annealed case. This is because the initial condition (21) leads to a bulky integral equation which does not appear to be solvable. Fig. 3 shows two examples of the optimal density history which we computed numerically for $\Lambda = 1$ and -1 , which correspond to $R/n_0 \simeq 1.52$ and 0.67 , respectively. We obtained these solutions by numerically solving Eq. (18) with the initial condition $Q(x, t = 0) = n_0/P(x, t = 0)$, where $P(x, t = 0)$ is given by Eq. (39), and then going back to the original density variable $q(x, t) = Q(x, t)P(x, t)$.

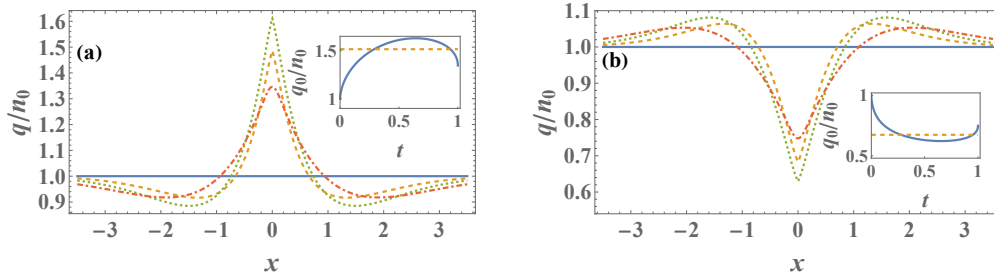


Figure 3: The optimal density history of the noninteracting RWs, for the quenched initial condition, as a function of x at times $t = 0, 0.25, 0.5$ and 1 (solid, dashed, dotted, and dash-dotted lines, respectively) for $\Lambda = 1$ (a) and $\Lambda = -1$ (b). Insets: The optimal densities at the origin, $q_0(t) = q(x = 0, t)$ (solid lines) and their time average values R (dashed lines).

As one can see, the optimal density history in the quenched case is markedly different from its counterpart in the annealed case. In particular, the density increase/decrease in the central region around $x = 0$ is accompanied by a gas depletion/excess in the surrounding regions. Such a visible redistribution of matter is absent in the annealed setting, see Fig. 2, where the gas has had an infinite time to equilibrate prior to $t = 0$. Similar mass redistribution phenomena were observed in the optimal paths of other large-deviation statistics in diffusive lattice gases with quenched initial conditions [37, 49]. Finally, in contrast to the annealed case, the optimal density history in the quenched case does not exhibit a time-reversal symmetry. On the other hand, there is still a corner singularity at $x = 0$ which persists at all times.

3.4. Connection with results of Ref. [22] for step-function initial density

For noninteracting RWs it is straightforward to extend our results for the uniform initial density to a step-function initial density,

$$\rho(x, t = 0) = \begin{cases} n_1, & x < 0, \\ n_2, & x > 0, \end{cases} \quad (43)$$

in both the annealed and quenched settings. To this end one can split the local time R to two parts, $R = R_1 + R_2$, where R_1 and R_2 are the contributions which come from particles whose initial positions were at $x < 0$ and $x > 0$, respectively.

Since the particles are noninteracting, R_1 and R_2 are statistically independent. As a result, the SCGF which describes the distribution of R is given by the sum of the SCGFs of R_1 and R_2 :

$$\mu(\Lambda) = \mu_1(\Lambda) + \mu_2(\Lambda), \quad (44)$$

because the cumulants of R are the sums of the cumulants of R_1 and of R_2 . In particular, it follows that the SCGF $\mu_{\text{full}}(\Lambda)$, which describes the homogeneous case $n_1 = n_2$, is related to the SCGF $\mu_{\text{half}}(\Lambda)$, which describes an initial density vanishing to the right of the origin (*i.e.* $n_2 = 0$), via

$$\mu_{\text{full}}(\Lambda) = 2\mu_{\text{half}}(\Lambda). \quad (45)$$

Therefore, using our results above for the homogenous case, one can obtain $\mu_{\text{half}}(\Lambda)$ and from it the corresponding rate function $s_{\text{half}}(R)$, and similarly for a general step-function initial condition (43).

The relation (45) enables us to directly compare our results for $s(R)$ with those of Ref. [22] which were obtained for the case $n_2 = 0$. Indeed, we find that for both the quenched and annealed initial conditions,

$$\mu(\Lambda) = -4n_0\phi\left(-\frac{\Lambda}{2}\right), \quad (46)$$

where the μ 's are the SCGFs μ_{full} obtained in the current work, and the ϕ 's are the functions given in Ref. [22]. The minus signs in (46) are due to different conventions in defining the Legendre transform, and the factors 4 and 1/2 are due to the factor of 2 in Eq. (45) and to our particular choice of diffusion coefficient $D_0 = 1$. With Eq. (46) at hand, one can check that our exact as well as asymptotic results for $s(R)$ for the non-interacting RWs agree³ with those of Ref. [22].

4. Typical fluctuations of local time in interacting lattice gases

For interacting lattice gases the time-dependent MFT equations can be solved exactly only in exceptional cases [50–52]. Quite often, however, MFT

³The $R \gg 1$ asymptotic of $s(R)$ in the annealed case, presented in Ref. [22], includes an additional constant term beyond what we have given in the third line of Eq. (34). This term, however, appears to be an excess of accuracy.

problems are amenable to an asymptotic solution in terms of a systematic expansion of the fields $q(x, t)$ and $p(x, t)$ in the powers of Λ :

$$\begin{aligned} q(x, t) &= n_0 + \Lambda q_1(x, t) + \Lambda^2 q_2(x, t) + \dots, \\ p(x, t) &= \Lambda p_1(x, t) + \Lambda^2 p_2(x, t) + \dots. \end{aligned} \quad (47)$$

In practice, this expansion procedure allows one to obtain first several distribution cumulants, and it has been used in the studies of several large-deviation problems for lattice gases, see *e.g.* [53–55].

For a uniform initial density, like in the present problem, these calculations become quite simple in the first order of the perturbation theory, where they give the second cumulant of R , that is the variance. Indeed, in the first order in Λ Eqs. (16) and (17) become

$$\partial_t q_1 = D(n_0) \partial_x^2 q_1 - \sigma(n_0) \partial_x^2 p_1, \quad (48)$$

$$\partial_t p_1 = -D(n_0) \partial_x^2 p_1 - \delta(x). \quad (49)$$

In what follows we will denote for brevity $D(n_0) \equiv D_0$ and $\sigma(n_0) \equiv \sigma_0$. As one can see, Eq. (49) is decoupled from Eq. (48), and it can be straightforwardly solved backward in time with the “initial” condition (8). The result is

$$p_1(x, t) = \frac{\Lambda}{2D_0} \left[x \operatorname{erf} \left(\frac{x}{\sqrt{4D_0(1-t)}} \right) + \frac{\sqrt{4D_0(1-t)} e^{-\frac{x^2}{4D_0(1-t)}}}{\sqrt{\pi}} - |x| \right]. \quad (50)$$

With this solution at hand, we can determine the action from the linearized version of Eq. (13),

$$s_{\text{dyn1}} = \frac{1}{2} \Lambda^2 \sigma(n_0) \int_0^1 dt \int_{-\infty}^{\infty} dx (\partial_x p_1)^2. \quad (51)$$

Using Eq. (50), we calculate

$$(\partial_x p_1)^2 = \frac{\Lambda^2}{4D_0^2} \operatorname{erfc}^2 \left(\frac{|x|}{\sqrt{4D_0(1-t)}} \right), \quad (52)$$

substitute this expression into Eq. (51), and evaluate the double integral. The resulting dynamical action in terms of Λ ,

$$s_{\text{dyn1}}(\Lambda) = \frac{(2 - \sqrt{2}) \sigma_0 \Lambda^2}{3\sqrt{\pi} D_0^{3/2}}, \quad (53)$$

combined with the relation $ds/dR = \Lambda$, yields our final result for the quadratic asymptotic of the action for the quenched initial condition:

$$s_{\text{quenched}}(R) = \frac{3\sqrt{\pi}D_0^{3/2}}{4(2 - \sqrt{2})\sigma_0} (R - n_0)^2, \quad (54)$$

for $|R - n_0| \ll n_0$. For the noninteracting RWs, with $D_0 = 1$ and $\sigma_0 = 2n_0$ (see Table 1), the r.h.s. of Eq. (54) coincides with the middle line of Eq. (42), as to be expected.

The (rescaled) variance of R can be immediately read off from Eq. (54):

$$\text{Var}_R^{\text{quenched}} = \frac{2(2 - \sqrt{2})\sigma_0}{3\sqrt{\pi}D_0^{3/2}}. \quad (55)$$

For the annealed initial condition we should also take into account the free-energy ‘‘cost’’ of the initial condition, see Eq. (14). Expanding Eq. (11) up to, and including, the second order in Λ , and plugging the result into Eq. (14), we obtain

$$s_{\text{in1}}(\Lambda) = \frac{1}{2}F''(n_0)\Lambda^2 \int_{-\infty}^{\infty} q_1^2(x, t=0) dx. \quad (56)$$

To determine $q_1(x, t=0)$, we linearize the initial condition (10) for the annealed case, which gives

$$q_1(x, t=0) = \frac{1}{F''(n_0)}p_1(x, t=0). \quad (57)$$

Therefore,

$$s_{\text{in1}}(\Lambda) = \frac{\Lambda^2}{2F''(n_0)} \int_{-\infty}^{\infty} p_1^2(x, t=0) dx. \quad (58)$$

Using the expression (50) at $t=0$ and evaluating the integral (58), we obtain

$$s_{\text{in1}} = \frac{(\sqrt{2} - 1)\sigma_0\Lambda^2}{3\sqrt{\pi}D_0^{3/2}}, \quad (59)$$

where we used the relation $F''(r) = 2D(r)/\sigma(r)$. The total action in the annealed case is the sum of s_{dyn1} and s_{in1} , which gives the final result

$$s_{\text{annealed1}}(\Lambda) = \frac{\sigma_0\Lambda^2}{3\sqrt{\pi}D_0^{3/2}} \quad (60)$$

or, in terms of R ,

$$s_{\text{annealed}}(R) = \frac{3\sqrt{\pi}D_0^{3/2}}{4\sigma_0} (R - n_0)^2, \quad (61)$$

for $|R - n_0| \ll n_0$. To remind the reader, $D_0 \equiv D(n_0)$ and $\sigma_0 \equiv \sigma(n_0)$. For the noninteracting RWs Eq. (61) coincides with the middle line of Eq. (34).

The rescaled variance in the annealed case,

$$\text{Var}_R^{\text{annealed}} = \frac{2\sigma_0}{3\sqrt{\pi}D_0^{3/2}}, \quad (62)$$

is larger than the variance (55) for the quenched initial condition. This is to be expected: the additional degrees of freedom at $t = 0$ facilitate fluctuations.

To conclude this Section, we present our results for the variance in the original, non-rescaled, variables:

$$\text{Var}_R^{\text{quenched}} = \frac{2(2 - \sqrt{2})\sigma_0}{3\sqrt{\pi}D_0^{3/2}T^{1/2}}, \quad (63)$$

$$\text{Var}_R^{\text{annealed}} = \frac{2\sigma_0}{3\sqrt{\pi}D_0^{3/2}T^{1/2}}. \quad (64)$$

That is, for all lattice gases, the standard deviation of fluctuations of R around its expected value $\bar{R} = n_0$ goes down with time as $T^{-1/4}$.

5. Summary

To summarize, we studied the full distribution $\mathcal{P}(R)$ of the local time R spent at a given spatial point by particles of a one-dimensional lattice gas, assuming an initially uniform gas density. At times T much longer than the characteristic microscopic time of the model, the distribution $\mathcal{P}(R)$ exhibits a simple and universal scaling behavior (12). The large deviation function $s(R)$ depends on the underlying microscopic model of the lattice gas only through the transport coefficients $D(\rho)$ and $\sigma(\rho)$. It also depends on the type of initial condition (quenched or annealed) and, in the one-dimensional setting, this dependence persists forever.

For a gas of noninteracting RWs we calculated $s(R)$ exactly by applying the MFT, thus re-deriving the results of Ref. [22] who obtained $s(R)$ in a

closely-related step-like setting via a microscopic solution of the model of non-interacting Brownian particles. In addition, the MFT equations provide a valuable information about the most likely history of the gas density $q(x, t)$ conditioned on a given value of R . This history dominates the contribution to $\mathcal{P}(R)$. For the RWs we obtained $q(x, t)$ analytically for the annealed initial condition, and numerically for the quenched initial condition. We also showed how our results for $s(R)$ can be straightforwardly extended to the case where the initial densities to the left and right of the origin are not equal.

Further, using the MFT, we studied *typical* fluctuations of R for a general particle- or energy-conserving diffusive lattice gas, for both the quenched and annealed initial conditions. We did it by calculating the variance of R which depends on the gas properties only through the values of the gas diffusivity and mobility evaluated at the initial (uniform) density.

It would be very interesting, but challenging, to calculate the complete large deviation function $s(R)$ for interacting lattice gases. Recent advances, which exploited the integrability of closely-related MFT equations for the Kipnis-Marchioro-Presutti model [50, 52] and for the SEP [51], indicate that this might conceivably be possible in some special cases. If it is not possible to calculate $s(R)$ exactly, one could alternatively probe the $R \rightarrow 0$ and $R \rightarrow \infty$ tails of $s(R)$ for different lattice gas models, by applying asymptotic methods to the MFT equations, exploiting the additional small or large parameter R .

Acknowledgments

The authors thank P. L. Krapivsky for a useful discussion and acknowledge support from the Israel Science Foundation (ISF) through Grants No. 2651/23 (NRS) and No. 1499/20 (BM).

Appendix A. Derivation of MFT equations

Upon rescaling $t/T \rightarrow t$, $x/\sqrt{T} \rightarrow x$, Eqs. (1) and (2) become

$$\partial_t \rho = \partial_x \left[D(\rho) \partial_x \rho + T^{-1/4} \sqrt{\sigma(\rho)} \eta \right], \quad (\text{A.1})$$

where η is also rescaled, by $T^{-3/4}$, and is delta correlated in the rescaled time and space variables. One therefore finds that, at long times $T \gg 1$, the noise term becomes effectively weak.

Let us now derive the MFT equations (16) and (17) of the main text. The probability density of the (dimensionless) Gaussian white noise is

$$\mathcal{P}[\eta] \sim \exp\left(-\int_0^1 dt \int_{-\infty}^{\infty} dx \frac{\eta^2}{2}\right). \quad (\text{A.2})$$

Expressing η through ρ and j , we can therefore write the probability of a joint history of the latter two as $P[\rho, j] \sim e^{-\sqrt{T}s}$ with the action functional

$$s = \int_0^1 dt \int_{-\infty}^{\infty} dx \frac{[j + D(\rho) \partial_x \rho]^2}{2\sigma(\rho)}. \quad (\text{A.3})$$

Exploiting the large parameter $\sqrt{T} \gg 1$, we now evaluate $\mathcal{P}(R)$ by applying the saddle-point approximation to the path integral. Within this framework, $-\ln \mathcal{P}(R)/\sqrt{T}$ is, in the leading order, given by the minimum of the action functional s over all realizations of ρ and j , constrained on the initial condition for the density ρ , and on a given value of R . We incorporate the latter constraint via a Lagrange multiplier, *i.e.* we minimize the modified action

$$s_\Lambda = s - \Lambda R = \int_0^1 dt \int_{-\infty}^{\infty} dx \left\{ \frac{[j + D(\rho) \partial_x \rho]^2}{2\sigma(\rho)} - \Lambda \delta(x) \rho(x, t) \right\}, \quad (\text{A.4})$$

where Λ is a Lagrange multiplier whose value is ultimately set by the constraint $\int_0^1 \rho(x=0, t) dt = R$.

It is convenient to define a “potential” $\psi(x, t)$ such that

$$\rho = \partial_x \psi, \quad j = -\partial_t \psi. \quad (\text{A.5})$$

(The existence of such a potential is guaranteed by the continuity equation.) Rerwriting the modified action as a functional of ψ , we obtain

$$\begin{aligned} s_\Lambda &= \int_0^1 dt \int_{-\infty}^{\infty} dx \left\{ \frac{[D(\partial_x \psi) \partial_x^2 \psi - \partial_t \psi]^2}{2\sigma(\partial_x \psi)} - \Lambda \delta(x) \partial_x \psi(x, t) \right\} \\ &= \int_0^1 dt \int_{-\infty}^{\infty} dx \left\{ \frac{1}{2} \sigma(\partial_x \psi) (\partial_x p)^2 + \Lambda \delta'(x) \psi(x, t) \right\}, \end{aligned} \quad (\text{A.6})$$

where we integrated by parts and defined the momentum density gradient

$$\partial_x p = \frac{D(\partial_x \psi) \partial_x^2 \psi - \partial_t \psi}{\sigma(\partial_x \psi)}. \quad (\text{A.7})$$

To minimize s_A , we calculate its variation with respect to a small variation of ψ ,

$$\begin{aligned} \delta s_A = & \int_0^1 dt \int_{-\infty}^{\infty} dx \left\{ -\frac{1}{2} \sigma' (\partial_x \psi) (\partial_x p)^2 \partial_x \delta \psi \right. \\ & \left. + (\partial_x p) [D' (\partial_x \psi) \partial_x^2 \psi \partial_x \delta \psi + D (\partial_x \psi) \partial_x^2 \delta \psi - \partial_t \delta \psi] + \Lambda \delta' (x) \delta \psi (x, t) \right\}. \end{aligned} \quad (\text{A.8})$$

To get rid of the derivatives from the terms proportional to $\delta \psi$, we integrate by parts in time or space. This yields $\delta s_A = \delta s_A|_{\text{bulk}} + \delta s_A|_{\text{boundary}}$ where the bulk term is

$$\begin{aligned} \delta s_A|_{\text{bulk}} = & \int_0^1 dt \int_{-\infty}^{\infty} dx \left\{ \partial_x \left[\frac{1}{2} \sigma' (\partial_x \psi) (\partial_x p)^2 \right] - \partial_x [(\partial_x p) D' (\partial_x \psi) \partial_x^2 \psi] \right. \\ & \left. + \partial_x^2 [(\partial_x p) D (\partial_x \psi)] + \partial_{xt} p + \Lambda \delta' (x) \right\} \delta \psi. \end{aligned} \quad (\text{A.9})$$

The boundary terms from the spatial integration by parts all vanish, while the temporal integration by parts yields a term

$$\delta s_A|_{\text{boundary}} = - \int_{-\infty}^{\infty} dx [\partial_x p \delta \psi]_{t=0}^{t=1}. \quad (\text{A.10})$$

We now require δs_A to vanish for variations $\delta \psi(x, t)$ at arbitrary $-\infty < x < \infty$ and $t > 0$. For the bulk term, this requirement yields the equation

$$\partial_t v = \partial_x \left[-D (q) \partial_x v - \frac{1}{2} \sigma' (q) v^2 \right] - \Lambda \delta' (x) \quad (\text{A.11})$$

where $v = \partial_x p$ and $q(x, t)$ is the optimal realization of the density $\rho(x, t)$. After a spatial integration, this equation yields the second MFT equation, Eq. (17) in the main text. The first MFT equation, Eq. (16) in the main text, follows from a spatial integration of the definition (A.7) of the momentum density.

Let us now derive the boundary conditions for the MFT equations. Requiring that the $t = 1$ term in Eq. (A.10) vanish for arbitrary $\delta \psi$, we obtain $\partial_x p (x, t = 1) = 0$, which after a spatial integration yields Eq. (8) of the main text. The initial condition for the quenched case is particularly simple. Here, $\rho(x, t = 0)$ is specified, so for the uniform-density initial condition, considered in the present paper, one simply has $q(x, t = 0) = n_0$, which is Eq. (9)

of the main text. The annealed case is slightly more tricky. Here, the initial density $\rho_0(x) = \rho(x, t = 0)$ is assumed to have equilibrated before time $t = 0$, and is therefore randomly sampled from the equilibrium distribution

$$\mathcal{P}[\rho_0(x)] \sim e^{-\int_{-\infty}^{\infty} dx \mathcal{F}[\rho_0(x)]}, \quad (\text{A.12})$$

where the function $\mathcal{F}(r)$ is given by Eq. (11) of the main text. As a result, in the minimization problem defined above, one must add to the action s_A an additional term,

$$s_{\text{in}} = \int_{-\infty}^{\infty} dx \mathcal{F}[\rho(x, 0)] = \int_{-\infty}^{\infty} dx \mathcal{F}[\partial_x \psi(x, 0)], \quad (\text{A.13})$$

which corresponds to the ‘‘cost’’ of the initial condition. The variation of this term is

$$\delta s_{\text{in}} = \int_{-\infty}^{\infty} dx \mathcal{F}'[\rho(x, 0)] \delta \rho(x, 0) = - \int_{-\infty}^{\infty} dx \partial_x \{ \mathcal{F}'[\partial_x \psi(x, 0)] \} \delta \psi(x, 0). \quad (\text{A.14})$$

The initial condition is then obtained by requiring that the sum of δs_{in} and the $t = 0$ term in Eq. (A.10),

$$\int_{-\infty}^{\infty} dx \partial_x \{ p(x, t = 0) - \mathcal{F}'[\partial_x \psi(x, 0)] \} \delta \psi(x, 0) = 0, \quad (\text{A.15})$$

vanishes for arbitrary variations $\delta \psi(x, 0)$, yielding that $\mathcal{F}'[\partial_x \psi(x, 0)] - p(x, t = 0)$ is a constant. This constant, however, must vanish, due to the condition $\mathcal{F}'(n_0) = 0$ and the vanishing boundary conditions at $|x| \rightarrow \infty$, thus yielding

$$p(x, t = 0) = \mathcal{F}'[\partial_x \psi(x, 0)], \quad (\text{A.16})$$

which is Eq. (10) of the main text.

Once the MFT problem is solved, the probability of observing a given R is given by $\mathcal{P}(R) \sim e^{-\sqrt{T}s}$, where s is the action (A.3) evaluated on the solution to the MFT equations which corresponds to the given R . Plugging Eq. (A.7) into (A.3), one obtains the following expression for s :

$$s = \frac{1}{2} \int_0^1 dt \int_{-\infty}^{\infty} dx \sigma(q) (\partial_x p)^2, \quad (\text{A.17})$$

which is Eq. (13) in the main text.

Appendix B. Evaluation of the integral (30) which gives $R(\Lambda)$ for the annealed case

Let us denote the integral which appears in Eq. (30) by

$$I(A) = \int_0^1 dt \operatorname{erfc}(A\sqrt{1-t}) \operatorname{erfc}(A\sqrt{t}), \quad (\text{B.1})$$

where $A = -\Lambda/2$. We now take the derivative under the integration sign in (B.1) to obtain

$$\begin{aligned} I'(A) &= \int_0^1 dt \left[-\frac{2\sqrt{t}e^{-A^2t}\operatorname{erfc}(A\sqrt{1-t})}{\sqrt{\pi}} - \frac{2\sqrt{1-t}e^{-A^2(1-t)}\operatorname{erfc}(A\sqrt{t})}{\sqrt{\pi}} \right] \\ &= \int_0^1 dt \left[-2\frac{2\sqrt{t}e^{-A^2t}\operatorname{erfc}(A\sqrt{1-t})}{\sqrt{\pi}} \right] \\ &= \frac{2}{A^3} \left[\frac{e^{-A^2}(2A - \sqrt{\pi}(A^2 + 1))}{\sqrt{\pi}} + \operatorname{erfc}(A) \right], \end{aligned} \quad (\text{B.2})$$

where, when moving from the first line to the second line in Eq. (B.2), we reversed the time $t \rightarrow 1-t$ in the second integral. Integrating Eq. (B.2) with respect to A we get

$$I(A) = 2 - \frac{2A^2\operatorname{erf}(A) - \frac{e^{-A^2}(\sqrt{\pi}-2A)}{\sqrt{\pi}} + \operatorname{erfc}(A)}{A^2} \quad (\text{B.3})$$

where we used that $I(0) = 1$ [which follows immediately from (B.1)]. And now finally we have [using Eq. (30)]

$$R(\Lambda) = n_0 e^{\frac{\Lambda^2}{4}} I\left(-\frac{\Lambda}{2}\right) = \frac{2n_0}{\Lambda^2} \left\{ e^{\frac{\Lambda^2}{4}} (\Lambda^2 - 2) \left[\operatorname{erf}\left(\frac{\Lambda}{2}\right) + 1 \right] + \frac{2\Lambda}{\sqrt{\pi}} + 2 \right\}, \quad (\text{B.4})$$

which is Eq. (31) of the main text.

Appendix C. Asymptotic behaviors of $s(\mathbf{R})$ in the annealed case

At $\Lambda \rightarrow \infty$, Eqs. (31) and (33) become $\bar{R} = R/n_0 \simeq 4/\Lambda^2$ and $\bar{s} = s/n_0 \simeq 4/\sqrt{\pi} + 8/\Lambda$, which together yield the first line in Eq. (34) of the main text.

At $\Lambda \rightarrow 0$, one finds $\bar{R} \simeq 1 + 4\Lambda/(3\sqrt{\pi})$, $\bar{s} \simeq 2\Lambda^2/(3\sqrt{\pi})$ which yield the middle line in Eq. (34). At $\Lambda \rightarrow \infty$, Eqs. (31) and (33) become

$$\bar{R} \simeq \left(4 - \frac{8}{\Lambda^2}\right) e^{\Lambda^2/4}, \quad (\text{C.1})$$

$$\bar{s} \simeq \left(4\Lambda - \frac{16}{\Lambda}\right) e^{\Lambda^2/4}, \quad (\text{C.2})$$

respectively. Inverting the relation (C.1) perturbatively at $R \gg 1$, we find that $\Lambda \simeq 2\sqrt{\ln\left(\frac{\bar{R}}{4}\right)} + \frac{1}{2\ln^{3/2}\left(\frac{\bar{R}}{4}\right)}$. Using these relations in (C.2), we find that

$$\bar{s} \simeq \Lambda\bar{R} - \frac{2\bar{R}}{\Lambda} \simeq 2\bar{R} \left[\sqrt{\ln\left(\frac{\bar{R}}{4}\right)} - \frac{1}{2\sqrt{\ln\left(\frac{\bar{R}}{4}\right)}} \right], \quad (\text{C.3})$$

which is the third line in Eq. (34) of the main text.

References

- [1] G. Wilemski and M. Fixman, J. Chem. Phys. **58**, 4009 (1973).
- [2] O. Benichou, M. Coppey, J. Klafter, M. Moreau and G. Oshanin, J. Phys. A: Math. Gen. **38**, 7205 (2005).
- [3] M. Doi, Chem. Phys., **11**, 107 (1975).
- [4] S. I. Temkin and B. I. Yakobson, J. Phys. Chem. **88**, 2679 (1984).
- [5] P. Lévy, Compositio Mathematica 7, **283** (1940).
- [6] S. Redner, *A Guide to First-Passage Processes* (Cambridge University Press 2001).
- [7] P. Tsobgni Nyawo, H. Touchette, Europhys. Lett. **116**, 50009 (2016).
- [8] P. Tsobgni Nyawo, H. Touchette, Phys. Rev. E **98**, 052103 (2018).
- [9] T. Agranov, P. L. Krapivsky, and B. Meerson, Phys. Rev. E **99**, 052102 (2019).

- [10] A. Pal, I. P. Castillo and A. Kundu, Phys. Rev. E **100**, 042128 (2019).
- [11] S. Mukherjee and N. R. Smith, Phys. Rev. E **107**, 064133, (2023).
- [12] S. N. Majumdar and A. Comtet, Phys. Rev. Lett. **89**, 060601 (2002).
- [13] S. Sabhapandit, S. N. Majumdar and A. Comtet, Phys. Rev. E **73**, 051102 (2006).
- [14] G. Kishore and A. Kundu, arXiv:2010.06262
- [15] S. Carmi, L. Turgeman and E. Barkai, J. Stat. Phys. **141**, 1071 (2010).
- [16] G. Louchard, J. Appl. Probab. **21**, 479 (1984).
- [17] M. Csorgo, Z. Shi and M. Yor, Bernoulli **5**, 1035 (1999).
- [18] D. S. Grebenkov, Phys. Rev. E **76**, 041139 (2007).
- [19] A. Comtet, J. Desbois and S. N. Majumdar, J. Phys. A: Math. Gen. **35**, L687 (2002).
- [20] A. Pal, R. Chatterjee, S. Reuveni and Anupam Kundu, J. Phys. A: Math. Theor. **52**, 264002 (2019).
- [21] P. Singh and A. Kundu, Phys. Rev. E **103**, 042119 (2021).
- [22] I. N. Burenev, S. N. Majumdar, and A. Rosso, arXiv:2306.16882.
- [23] L. Bertini, A. De Sole, D. Gabrielli, G. Jona-Lasinio, and C. Landim, Rev. Mod. Phys. **87**, 593 (2015).
- [24] P. I. Hurtado and P. L. Garrido, Phys. Rev. Lett. **102**, 250601 (2009).
- [25] P. I. Hurtado and P. L. Garrido, Phys. Rev. Lett. **107**, 180601 (2011).
- [26] V. Lecomte, J. P. Garrahan, and F. van Wijland, J. Phys. A: Math. Theor. **45**, 175001 (2012).
- [27] G. Bunin, Y. Kafri, and D. Podolsky, Europhys. Lett. **99**, 20002 (2012).
- [28] A. K. Hartmann, B. Meerson, and P. Sasorov, Phys. Rev. Res. **1**, 032043 (R) (2019).

- [29] A. K. Hartmann, B. Meerson and P. Sasorov, Phys. Rev. E **104**, 054125 (2021).
- [30] A. K. Hartmann and B. Meerson, arXiv:2310.14003.
- [31] H. Spohn, *Large Scale Dynamics of Interacting Particles* (Springer, New York, 1991).
- [32] T. M. Liggett, *Stochastic Interacting Systems: Contact, Voter, and Exclusion Processes* (Springer, New York, 1999).
- [33] C. Kipnis and C. Landim, *Scaling Limits of Interacting Particle Systems* (Springer, New York, 1999).
- [34] P. L. Krapivsky, S. Redner, and E. Ben-Naim, *A Kinetic View of Statistical Physics* (Cambridge University Press, Cambridge, UK, 2010).
- [35] C. Kipnis, C. Marchioro, and E. Presutti, J. Stat. Phys. **27**, 65 (1982).
- [36] M. R. Evans and T. Hanney, J. Phys. A: Math. Gen. **38** R195 (2005).
- [37] P. L. Krapivsky, B. Meerson, and P. V. Sasorov, J. Stat. Mech. (2012) P12014.
- [38] S. Katz, J. L. Lebowitz, and H. Spohn, J. Stat. Phys. **34**, 497 (1984).
- [39] Y. Baek, Y. Kafri, and V. Lecomte, Phys. Rev. Lett. **118**, 030604 (2017).
- [40] W. Kob and H. C. Andersen, Phys. Rev. E **48**, 4364 (1993).
- [41] C. Arita, P. L. Krapivsky, and K. Mallick, J. Phys. A: Math. Theor. **51**, 125002 (2018).
- [42] P. L. Krapivsky, J. Stat. Mech. P06012 (2013).
- [43] D. Gabrielli and P. L. Krapivsky, J. Stat. Mech. (2018) 043212.
- [44] B. Derrida and A. Gerschenfeld, J. Stat. Phys. **137**, 978 (2009).
- [45] A. D. Polyanin and A. V. Manzhirov, *Handbook of Integral Equations, Second Edition* (Chapman and Hall/CRC, New York, 1998).
- [46] F. D. Cunden, P. Facchi, and P. Vivo, J. Phys. A: Math. Theor. **49**, 053303 (2016).

- [47] R. A. Blythe and A. J. Bray, Phys. Rev. E **67**, 041101 (2003).
- [48] B. Meerson, A. Vilenkin, and P. L. Krapivsky, Phys. Rev. E **90**, 022120 (2014).
- [49] B. Meerson and P. V. Sasorov, Phys. Rev. E **89**, 010101(R) (2014).
- [50] E. Bettelheim, N. R. Smith, and B. Meerson, Phys. Rev. Lett. **128**, 130602 (2022).
- [51] K. Mallick, H. Moriya, and T. Sasamoto, Phys. Rev. Lett. **129**, 040601 (2022).
- [52] E. Bettelheim, N. R. Smith, and B. Meerson, J. Stat. Mech. (2022) 093103.
- [53] P. L. Krapivsky and B. Meerson, Phys. Rev. E **86**, 031106 (2012).
- [54] P. L. Krapivsky, K. Mallick, and T. Sadhu, Phys. Rev. Lett. **113**, 078101 (2014).
- [55] P. L. Krapivsky, K. Mallick, and T. Sadhu, J. Stat. Phys. **160**, 885 (2015).